# Raman Spectroscopy of DNA-Metal Complexes. I. Interactions and Conformational Effects of the Divalent Cations: Mg, Ca, Sr, Ba, Mn, Co, Ni, Cu, Pd, and Cd[1]

John Duguid,[‡] Victor A. Bloomfield,[‡] James Benevides,[§] and George J. Thomas, Jr.[§]

[‡]Department of Biochemistry, University of Minnesota, St. Paul, Minnesota 55108, and [§]Division of Cell Biology and Biophysics, School of Biological Sciences, University of Missouri–Kansas City, Kansas City, Missouri 64110 USA

ABSTRACT Interactions of divalent metal cations ($Mg^{2+}$, $Ca^{2+}$, $Ba^{2+}$, $Sr^{2+}$, $Mn^{2+}$, $Co^{2+}$, $Ni^{2+}$, $Cu^{2+}$, $Pd^{2+}$, and $Cd^{2+}$) with DNA have been investigated by laser Raman spectroscopy. Both genomic calf-thymus DNA (>23 kilobase pairs) and mononucleosomal fragments (160 base pairs) were employed as targets of metal interaction in solutions containing 5 weight-% DNA and metal:phosphate molar ratios of 0.6:1. Raman difference spectra reveal that transition metal cations ($Mn^{2+}$, $Co^{2+}$, $Ni^{2+}$, $Cu^{2+}$, $Pd^{2+}$, and $Cd^{2+}$) induce the greatest structural changes in B-DNA. The Raman (vibrational) band differences are extensive and indicate partial disordering of the B-form backbone, reduction in base stacking, reduction in base pairing, and specific metal interaction with acceptor sites on the purine (N7) and pyrimidine (N3) rings. Many of the observed spectral changes parallel those accompanying thermal denaturation of B-DNA and suggest that the metals link the bases of denatured DNA. While exocyclic carbonyls of dT, dG, and dC may stabilize metal ligation, correlation plots show that perturbations of the carbonyls are mainly a consequence of metal-induced denaturation of the double helix. Transition metal interactions with the DNA phosphates are weak in comparison to interactions with the bases, except in the case of $Cu^{2+}$, which strongly perturbs both base and phosphate group vibrations. On the other hand, the Raman signature of B-DNA is largely unperturbed by $Mg^{2+}$, $Ca^{2+}$, $Sr^{2+}$, and $Ba^{2+}$, suggesting much weaker interactions of the alkaline earth metals with both base and phosphate sites. A notable exception is a moderate perturbation by alkaline earths of purine N7 sites in 160-base pair DNA, with $Ca^{2+}$ causing the greatest effect. Correlation plots demonstrate a strong interrelationship between perturbations of Raman bands assigned to ring vibrations of the bases and those of bands assigned to exocyclic carbonyls and backbone phosphodiester groups. However, strong correlations do not occur between the Raman phosphodioxy band (centered near 1092 $cm^{-1}$) and other Raman bands, suggesting that the former is not highly sensitive to the structural changes induced by divalent metal cations.

The structural perturbations induced by divalent cations are much greater for >23-kilobase pair DNA than for 160-base pair DNA, as evidenced by both the Raman difference spectra and the tendency toward the formation of insoluble aggregates. In the presence of transition metals, aggregation of high-molecular-weight DNA is evident at temperatures as low as 11°C. A relationship between DNA melting and aggregation is proposed in which initial metal binding at major groove sites locally destabilizes the B-DNA double helix, causing displacement of the bases away from one another and exposing additional metal binding sites. Metal cation linkage of two displaced bases would allow separate DNA strands to crosslink. Aggregation is proposed to result from the formation of an extended network of these crosslinks.

## INTRODUCTION

Divalent metal cations may alter DNA structure by inducing any of the following: helix-to-coil transitions (Dove and Davidson, 1962; Eichhorn and Clark, 1965; Eichhorn and Shin, 1968; Shin and Eichhorn, 1968; Dix and Strauss, 1972), right- to left-handed helical transitions in alternating GC sequences (Jovin et al., 1983; Gessner et al., 1985; Theophanides and Tajmir-Riahi, 1985; Woisard et al., 1985; Jovin et al., 1987; Keller and Hartman, 1987; Keller et al., 1988), multistranded helical complexes in guanine tandem repeats (Hardin et al., 1992), nonspecific aggregation at elevated temperatures (Knoll et al., 1988), and condensation of the polynucleotide chain in solutions of low dielectric constant (Wilson and Bloomfield, 1979; Votavov et al., 1986). The ability of a divalent metal cation to influence DNA structure makes it a potential modulator of DNA function. It is therefore important to identify the metal-ion binding sites of DNA and determine how binding may affect secondary and tertiary structures.

DNA-metal cation interactions and their effects on DNA structure have been investigated by a variety of techniques, including sedimentation equilibrium measurements (Zimmer et al., 1974), UV-visible spectrophotometry (Dove and Davidson, 1962; Eichhorn and Clark, 1965; Eichhorn and Shin, 1968; Shin and Eichhorn, 1968; Dix and Strauss, 1972; Luck and Zimmer, 1972; Zimmer et al., 1974), circular dichroism spectroscopy (Luck and Zimmer, 1972; Clement et al., 1973; Zimmer et al., 1974; Jovin et al., 1983; Woisard et al., 1985), vibrational spectroscopy (Yamane and Davidson, 1961; Keller and Hartman, 1986, 1987; Day et al., 1988; Keller et al., 1988; Tajmir-Riahi et al., 1988; Langlais et al., 1990) and NMR spectroscopy (Rose et al., 1980; Van Steenwinkel et al., 1981; Granot and Kearns, 1982; Granot et al., 1982; Rose et al., 1982; Chang and Kearns, 1986; Kennedy and Bryant, 1986). Collectively, these studies indicate that the metal ions bind preferentially to the bases relative to phosphates in the following order: $Hg^{2+} > Cu^{2+} > Pb^{2+} > Cd^{2+} > Zn^{2+} > Mn^{2+} > Ni^{2+}$, $Co^{2+} > Fe^{2+}$

*Received for publication 22 March 1993 and in final form 2 August 1993.*

Address reprint requests to Dr. Victor A. Bloomfield or Dr. George J. Thomas, Jr.

[1] Part XLIV in the series, Raman Spectral Studies of Nucleic Acids.



0006-3495/93/11/1916/13 $2.00

> $Ca^{2+}$ > $Mg^{2+}$, $Ba^{2+}$. Metals with the strongest base affinity apparently perturb hydrogen bonding between base pairs, thus destabilizing the B form of DNA and stabilizing alternative structural forms. Conversely, cations with greater binding specificity for the phosphates stabilize B-DNA, apparently through charge neutralization of the sugar-phosphate backbone. Except for $Hg^{2+}$ (Yamane and Davidson, 1961; Keller and Hartman, 1986), metal cations bind preferentially to GC rather than AT regions. The N7 site of guanine is also recognized as an important site of metal interaction and is often implicated in chelation with a nearby phosphate group (Clement et al., 1973; Sissf et al., 1976; Van Steenwinkel et al., 1981).

Vibrational spectroscopy (both infrared and Raman) has the capability of revealing metal binding sites in high-molecular-weight DNA and large nucleoprotein assemblies. Day et al. (1988) used Raman spectroscopy to examine the effects of $Hg^{2+}$ on the filamentous viruses fd and Pf1 and found two distinct modes of $Hg^{2+}$ binding to bases of the packaged single-strand DNA. $Hg^{2+}$ forms bridges between antiparallel strands of DNA in fd but not in Pf1. Keller and co-workers (Keller and Hartman, 1987; Keller et al., 1988) employed infrared spectroscopy to demonstrate interactions of $Hg^{2+}$ and $Cd^{2+}$ with acceptor sites of guanine residues in poly(dG-dC)·poly(dG-dC). These interactions induce stabilization of the left-handed Z form of the polynucleotide at Hg(II):nucleotide and Cd(II):nucleotide ratios of 1:5 and 2:5, respectively. Fourier transform infrared studies on calf thymus DNA (Theophanides and Tajmir-Riahi, 1985) in the presence of $Cu^{2+}$ and $Mg^{2+}$ show that these metals are also capable of stabilizing Z-DNA. The use of Raman spectroscopy (Tajmir-Riahi et al., 1988; Langlais et al., 1990) to investigate interactions of $Cu^{2+}$, $Pb^{2+}$, $Zn^{2+}$, $Cd^{2+}$, $Mg^{2+}$, and $Ca^{2+}$ with calf thymus DNA indicates the phosphates as targets of each cation. $Cu^{2+}$ also interacts strongly with G and C bases, thus disrupting the double helix, while $Zn^{2+}$ and $Cd^{2+}$ interact preferentially with N7 of guanine or N3 of cytosine. $Mg^{2+}$, $Ca^{2+}$, and, surprisingly, $Pb^{2+}$ were found to interact very weakly with the bases. The vibrational spectra thus confirm that transition metals tend to have higher affinities for the DNA bases, while alkaline earths have higher affinities for the phosphates.

Here we employ Raman spectroscopy to assess nucleic acid binding sites and to characterize and compare the perturbations to DNA secondary and tertiary structures induced in DNA by alkaline earth ions ($Sr^{2+}$, $Ba^{2+}$, $Mg^{2+}$, and $Ca^{2+}$) and transition metal ions ($Mn^{2+}$, $Co^{2+}$, $Ni^{2+}$, $Pd^{2+}$, $Cu^{2+}$, and $Cd^{2+}$). The large body of experimental data obtained in this study is synthesized into correlation plots that reveal relationships between perturbations of structure-sensitive Raman bands and the types of metal ions involved. For the present study we have utilized calf thymus DNA of two different sizes: a mononucleosomal fragment of 160 base pairs (bp) and genomic calf thymus DNA comprising fragments greater than 23 kbp. Our studies complement and extend previous investigations and reveal a consistent pattern of double helix denaturation by most divalent transition metal ions. These perturbations are consistently larger for the higher-molecular-weight DNA fragments. Alkaline earth metals, on the other hand, exert a relatively small effect on the stability of double helical DNA, irrespective of fragment size.

## MATERIALS AND METHODS

### Salt solutions

Chloride salts of strontium, barium, magnesium, manganese, cobalt, nickel, cadmium, copper, and palladium were obtained from Aldrich (Milwaukee, WI). Calcium chloride was obtained from EM Science (Darmstadt, Germany). Stock solutions containing 200 mM metal salt and 5 mM sodium cacodylate were adjusted to pH 6.5 with HCl. Solutions of copper and palladium chlorides, which formed insoluble hydroxides near neutral pH, were brought to pH values of 3.5 and 1.3, respectively, by the addition of HCl.

### Preparation of DNA

High-molecular-weight calf thymus DNA (Pharmacia) of >23 kbp was dissolved at 3 mg/ml in purified (Milli-Q) water and stirred overnight to obtain a uniform solution. One-third volume of Tris-saturated phenol was added, and the mixture was centrifuged at 12,500 rpm in a Beckman JA-20 rotor for 30 min at 0°C. The aqueous layer was removed and precipitated with ethanol. The precipitate was collected, washed with ethanol three or four times, resuspended in Milli-Q water, and allowed to stand overnight. The solution was dialyzed twice against 4 M NaCl plus 5 mM sodium EDTA (pH 7.5), twice against 0.4 M NaCl (pH 7.5), and four times against Milli-Q water and then lyophilized. The lyophilizate was desiccated at −20°C.

Mononucleosomal calf thymus DNA (160 ± 5 bp) was prepared using standard methods (Strzelecka and Rill, 1987; Wang et al., 1990) and purified by three successive phenol extractions. One and a half volumes of cold isopropanol (−20°C) was added to the aqueous DNA-containing layer, and the mixture was stored overnight at −20°C. The precipitated DNA was removed by centrifugation at 8000 rpm in a Beckman JA-10 rotor for 45 min, dried, and resuspended in 10 mM $Na_2HPO_4$ plus 0.2 M NaCl plus 1 mM EDTA (pH 7.5). The solution was dialyzed twice against 4 M NaCl plus 5 mM EDTA (pH 7.5), twice against 1 M NaCl (pH 7.5), and four times against Milli-Q water and then lyophilized. The lyophilizate was desiccated at −20°C.

### Preparation of samples for Raman spectroscopy

To prepare each metal-DNA complex, DNA was dissolved to 5% (w/w) in a solution containing 100 mM metal chloride plus 5 mM sodium cacodylate (pH 6.5), yielding a divalent-metal cation to phosphate ratio ($[M^{2+}]/[PO_2^-]$) of 0.6. Solutions were maintained overnight at 4°C. CuDNA and PdDNA were prepared using $CuCl_2$ and $PdCl_2$ solutions with initial pH values of 3.5 and pH 1.3, respectively, to avoid the formation of insoluble hydroxides. Upon reaction with DNA, the pH values equilibrated to 3.1 (CuDNA) and 1.7 (PdDNA). At room temperature, nucleosomal CoDNA, NiDNA, and CdDNA became slightly turbid. All metal complexes of high-molecular-weight DNA formed fibrous precipitates. DNA complexes were mixed to homogeneity, and 10-μl aliquots were sealed in glass capillary tubes (Kimax no. 34502) for Raman analysis.

Raman spectra were excited with the 514.5 nm line of an argon laser (Coherent Innova 70), using approximately 200 mW of radiant power at the sample. All samples were thermostated at 11°C during data collection. The spectra were collected on a triple spectrograph (Spex Instruments model 1877 Triplemate) equipped with an intensified diode array detector (EG&G Princeton Applied Research OMA-III). The effective spectral resolution was 8 $cm^{-1}$. Further description of this instrumentation is given elsewhere (Lamba et al., 1990). In order to improve Raman signal-to-noise ratios, up to several hundred accumulated spectra, each of 30 s exposure time, were averaged over the spectral interval 600–1720 $cm^{-1}$. In the interval 650–1650 $cm^{-1}$ of spectra reported below, the signal-to-noise level is 50:1 for the most

prominent Raman bands and correspondingly lower for bands of lesser intensity. Higher spectral noise is observed near the bandpass limits (600–650 and 1650–1720 $cm^{-1}$) because of less efficient focusing of the Raman scattered radiation near the edges of the diode array detector. Weak background scattering by the aqueous solvent was removed using computer subtraction techniques described previously (Benevides et al., 1984). Relative intensities of diagnostic DNA bands at 680, 786, 1014, 1578, and 1671 $cm^{-1}$ compare favorably with those obtained using a single-channel scanning Raman spectrophotometer (Prescott et al., 1984).

## Data analysis

Difference Raman spectra were computed in accordance with the procedure of Langlais et al. (1990) (i.e., difference spectrum = spectrum of DNA/metal complex minus spectrum of DNA). Spectra of DNA and complexes were collected consecutively, usually within an 18-h period for 23 kbp DNA, and within a 12-h period for 160 bp DNA. For normalization of minuend and subtrahend, we employed either the intense band at 786 $cm^{-1}$, assigned to overlapping modes of the cytosine ring and phosphodiester backbone, or the weaker band near 1014 $cm^{-1}$, assigned to the sugar moiety. The band near 1014 $cm^{-1}$ is one of the least sensitive to DNA melting and divalent metal binding. Several Raman bands exhibiting significant dependence of intensity and/or frequency upon metal-ion binding were identified from the difference spectra. The magnitude of intensity change was computed as the percentage change in the parent band of metal-free B-DNA. Absolute Raman intensity changes and the estimated uncertainties in their measurement were catalogued for bands (residue assignments) near 668 (dG and dT), 681 (dG), 727 (dA), 750 (dT), 834 (OPO), 1092 ($PO_2^-$), 1257 (dC), 1489 (dG, dA), and 1668 $cm^{-1}$ (C=O groups of dT, dG, dC). In certain complexes, the bands at 1092 and 1489 $cm^{-1}$ were observed to undergo frequency shifts, which complicates the measurement of their intensity changes. This leads to derivative type features in the difference spectra, the magnitudes of which are conveniently expressed as peak-to-trough distances. Accordingly, in the tabulations given below, the listed intensity changes of bands near 1092 and 1489 $cm^{-1}$ represent the combined effects of frequency shift and intensity perturbation.

Uncertainties associated with Raman band changes upon metal-DNA complexation were evaluated from the difference spectra. Applying the rule for additivity of variances, the total standard deviation, $\sigma_{tot}$, attributed to the perturbation of a particular band is given by the relation

$$\sigma_{tot} = (\sigma_\nu^2 + \sigma_{785}^2 + \sigma_0^2)^{1/2} \quad (1)$$

where $\sigma_\nu$, $\sigma_{785}$, and $\sigma_0$ are, respectively, the root-mean-square noise associated with the difference Raman band at frequency $\nu$, the reference normalization band at 785 $cm^{-1}$, and the baseline. The margin of error, which is given by $5.0 \times \sigma_{tot}$, represents 99.7% confidence that a band intensity is within $\pm 2.5 \times \sigma_{tot}$. The values expressed in Table 1 are determined as $\pm 2.5 \times \sigma_{tot}$.

We also documented the shift observed in the local maximum of the complex Raman band near 660–685 $cm^{-1}$, which is sensitive to sugar pucker and glycosyl torsion of deoxyguanosine nucleoside residues (Thomas and Benevides, 1985; Benevides et al., 1988; Thomas and Wang, 1988). In B-DNA, the complex band consists of a major component centered at 681 $\pm$ 2 $cm^{-1}$, which is diagnostic of C2′-*endo*/*anti* dG conformers (Benevides et al., 1988). This dG conformation marker is displaced to 665 $\pm$ 2 $cm^{-1}$ when dG is converted to the C3′-*endo*/*anti* conformation (Thomas and Wang, 1988). Thus, the Raman intensity ratio $I_{681}/I_{665}$ provides a measure of the distribution of dG residues between C2′-*endo*/*anti* and C3′-*endo*/*anti* conformations. We report below the changes observed in this intensity ratio upon formation of metal-DNA complexes. A considerably weaker dT component, centered near 665 $cm^{-1}$ in B-DNA (Thomas and Benevides, 1985), partially overlaps the dG conformation markers but does not preclude use of the $I_{681}/I_{665}$ intensity ratio as an approximate indicator of dG nucleoside conformations.

Similarly, we estimated the percentage of nucleotide residues retaining B-form backbone geometry in a metal-DNA complex using the relation

$$\%\text{B-form} = 100 \times (I_{834}^{MDNA} - I_{834}^{d})/(I_{834}^{DNA} - I_{834}^{d}) \quad (2)$$

where $I_{834}$ is the intensity of the B-form marker band near 834 $cm^{-1}$, assigned to coupled bond stretching vibrations of the phosphodiester 5′C-O-P-O-C3′ group (Erfurth et al., 1972; Erfurth and Peticolas, 1975; Benevides et al., 1991). The superscripts MDNA, DNA, and d refer, respectively, to

**TABLE 1 Perturbations of selected Raman bands of DNA in divalent metal complexes**

| Group: Data* | Backbone 100-$\%\delta_{834}$ | C=O $\%\delta$C=O | dC $\%\delta_{1257}$ | dG,dA $\lvert\%\delta_{1489}\rvert$ | dA $\%\delta_{727}$ | dG $\delta\sigma_{681}$ | dG $I_{681}/I_{665}$ | dT $\%\delta_{750}$ | $PO_2^-$ $\lvert\%\delta_{1092}\rvert$ |
|---|---|---|---|---|---|---|---|---|---|
| DNA‡ | 100 | | | | | | 1.5 | | |
| SrDNA‡ | 85 ± 9 | 9 ± 8 | 6 ± 5 | 3 ± 4 | −2 ± 9 | +1 | 1.5 | −3 ± 11 | 4 ± 4 |
| BaDNA‡ | 83 ± 10 | 10 ± 9 | 14 ± 6 | 13 ± 4 | −1 ± 10 | 0 | 1.3 | −7 ± 12 | 4 ± 5 |
| MgDNA‡ | 93 ± 9 | 12 ± 8 | 0 ± 5 | 13 ± 4 | −4 ± 8 | 0 | 1.5 | 1 ± 10 | 10 ± 4 |
| CaDNA‡ | 82 ± 12 | 15 ± 10 | 12 ± 7 | 19 ± 5 | 0 ± 11 | −1 | 1.3 | −1 ± 14 | 4 ± 5 |
| MnDNA‡ | 77 ± 11 | 13 ± 10 | 17 ± 6 | 23 ± 4 | 3 ± 11 | −1 | 1.3 | 0 ± 13 | 9 ± 5 |
| CdDNA‡ | 78 ± 13 | 36 ± 11 | 27 ± 8 | 22 ± 5 | 1 ± 13 | −3 | 1.3 | −2 ± 15 | 15 ± 6 |
| NiDNA‡ | 63 ± 8 | 24 ± 7 | 24 ± 4 | 21 ± 3 | 8 ± 7 | −4 | 1.1 | 3 ± 9 | 9 ± 4 |
| CoDNA‡ | 47 ± 14 | 36 ± 13 | 45 ± 8 | 28 ± 6 | 22 ± 14 | −5 | 1.0 | 1 ± 17 | 11 ± 7 |
| DNA§ | 100 | | | | | | 1.5 | | |
| SrDNA§ | 91 ± 21 | 20 ± 17 | −14 ± 13¶ | 9 ± 9 | −4 ± 21 | +2 | 1.4 | 1 ± 24 | 15 ± 10 |
| BaDNA§ | 82 ± 29 | 14 ± 23 | 24 ± 18‖ | 10 ± 12** | 3 ± 28 | +1 | 1.4 | −4 ± 33 | 15 ± 13 |
| MgDNA§ | 91 ± 19 | 13 ± 15 | −7 ± 12 | 9 ± 8 | −6 ± 18 | +1 | 1.3 | 6 ± 21 | 6 ± 9 |
| CaDNA§ | 83 ± 18 | 14 ± 15 | 6 ± 11 | 22 ± 8 | 0 ± 18 | 0 | 1.4 | −3 ± 21 | 9 ± 8 |
| MnDNA§ | 36 ± 14 | 58 ± 11 | 96 ± 9 | 37 ± 6 | 27 ± 14 | −11 | 0.8 | −4 ± 16 | 21 ± 7 |
| CdDNA§ | 41 ± 15 | 56 ± 12 | 83 ± 10 | 35 ± 7 | 18 ± 15 | −9 | 0.9 | −4 ± 18 | 19 ± 7 |
| NiDNA§ | 31 ± 13 | 71 ± 11 | 92 ± 8 | 43 ± 6 | 11 ± 13 | −8 | 1.0 | −9 ± 15 | 16 ± 6 |
| CuDNA§ | 45 ± 20 | 46 ± 21 | 77 ± 18 | 48 ± 12 | 19 ± 23 | −13 | 0.7 | 10 ± 27 | 54 ± 12 |
| PdDNA§ | 0 ± 17 | 106 ± 14 | 195 ± 11 | 70 ± 7 | 53 ± 17 | −14 | 0.7 | 42 ± 20 | 23 ± 8 |

* Symbols: $\delta$ and $\%\delta$ represent absolute and percentage changes, respectively, in band intensity. C=O is the complex carbonyl band in the 1650–1680 $cm^{-1}$ interval. $\delta\sigma$ is the absolute frequency ($cm^{-1}$) shift of the indicated band. $I$ represents peak height.

‡ Data collected at 11°C on 160 bp fragments of calf thymus DNA and its complexes.

§ Data collected at 11°C on >23 kbp fragments of calf thymus DNA and its complexes.

¶ Error does not include baseline drift, estimated as +14%.

‖ Error does not include baseline drift, estimated as −29%.

** Error does not include baseline drift, estimated as −9%.

the metal-DNA complex, to B-DNA in the absence of the metal, and to thermally denatured DNA. The correlation of Eq. 2 is based upon earlier work on model compounds (Erfurth et al., 1972; Erfurth and Peticolas, 1975; Prescott et al., 1984; Benevides et al., 1988; Thomas and Wang, 1988; Benevides et al., 1991).

## RESULTS

Fig. 1 shows the Raman spectrum of B-DNA in the interval 600–1720 $cm^{-1}$. Labels identify bands assigned to specific base, sugar, and phosphate group vibrations and their structural significance. More detailed analyses of related Raman spectra of DNA and metal complexes have been given (Lord and Thomas, 1967; Erfurth et al., 1972; Erfurth and Peticolas, 1975; Prescott et al., 1984; Thomas and Benevides, 1985; Benevides et al., 1988; Thomas and Wang, 1988; Tajmir-Riahi et al., 1988; Langlais et al., 1990; Benevides et al., 1991). Spectra-structure correlations of interest for this study are as follows: (*a*) The guanine nucleoside marker in the interval 620–685 $cm^{-1}$ is diagnostic of sugar pucker and glycosyl torsion of dG residues (Benevides et al., 1988; Thomas and Wang, 1988). (*b*) The band near 727 $cm^{-1}$ identifies the adenine residue, free of metal binding (Thomas and Benevides, 1985; Thomas and Wang, 1988). (*c*) The thymidine marker near 750 $cm^{-1}$ identifies C2′-*endo*/*anti* conformers of dT (Thomas and Benevides, 1985). (*d*) Bands in the region 800–1100 $cm^{-1}$ are generally sensitive to backbone geometry and secondary structure, especially the B-form marker near 834 $cm^{-1}$ (Erfurth et al., 1972; Prescott et al., 1984; Benevides, et al. 1991). (*e*) The $PO_2^-$ marker near 1092 $cm^{-1}$ is responsive to large changes in the electrostatic environment of the phosphate group (Aubrey et al., 1992; Stangret and Savoie, 1992). (*f*) Various bands in the 1200–1600 $cm^{-1}$ region, assigned to purine and pyrimidine ring vibrations, are sensitive indicators of ring electronic structures and are expected to exhibit perturbations upon metal binding at ring sites. Among the most informative of these are the band of guanine at 1489 $cm^{-1}$, which shifts upon binding of electrophilic agents ($H^+$, metal ions, etc.) to the N7 acceptor (Moller et al., 1980; Langlais et al., 1990), and bands at 1240 and 1257 $cm^{-1}$, which are highly hypochromic in B-DNA and gain appreciable intensity with DNA denaturation.

The band near 1240 $cm^{-1}$ is due predominantly to dT, but with a minor contribution from dC (Erfurth and Peticolas, 1975; Thomas and Benevides, 1985). The band near 1257 $cm^{-1}$ has been assigned to dC (Lord and Thomas, 1967; Benevides et al., 1991). Thermal denaturation of high-molecular-weight DNA results in a pronounced intensity increase at 1240 $cm^{-1}$ and a marginal intensity increase at 1257 $cm^{-1}$ (Erfurth and Peticolas, 1975; Benevides et al., 1991). This is consistent with extensive melting of AT-rich regions and limited melting of GC-rich regions. On the other hand, when denaturation results from binding of mercuric chloride, the 1257 $cm^{-1}$ band of dC undergoes a very large intensity increase (Lord and Thomas, 1967). By monitoring these two bands the effect of metal ion binding on dT and dC can be determined independently. (*g*) The broad band centered near 1668 $cm^{-1}$, assigned to coupled C=O stretching and N—H deformation modes of dT, dG, and dC, is sensitive to denaturation, reflecting altered hydrogen bonding states of the exocyclic donor and acceptor groups (Erfurth and Peticolas, 1975; Benevides et al., 1991).

Fig. 2 shows a comparison of the effects of alkaline earth and transition metals on the Raman spectra of high- and low-molecular-weight DNA. These spectra show that in the presence of alkaline earth metals there is very little change in the Raman spectrum of either high- or low-molecular-weight DNA. However, in the presence of transition metals, the DNA Raman signature is perturbed extensively, and the perturbations are amplified in the case of high-molecular-weight DNA. The most noticeable changes include a decrease in intensity at 834 $cm^{-1}$ and increases in intensity in the interval

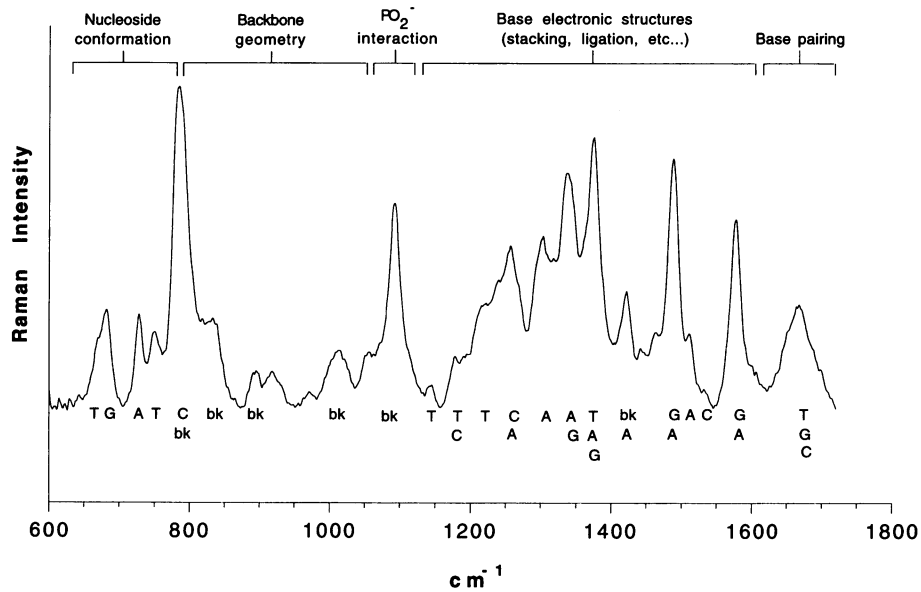


FIGURE 1 Raman spectrum of calf thymus DNA in the region 600–1800 $cm^{-1}$, showing sensitivity to various conformational features (top labels) and specific vibrational assignments to base (A, T, G, C) and backbone (bk) residues (bottom labels).

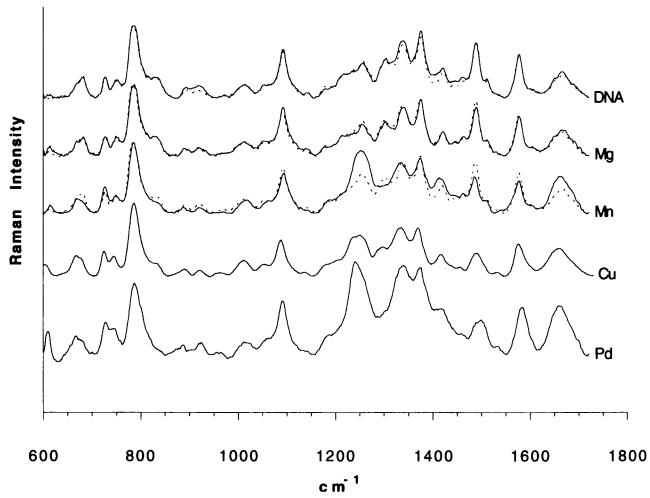


FIGURE 2 From top to bottom: Raman spectra of (sodium) calf thymus DNA in the absence of other metals (DNA), in the presence of an alkaline earth metal (Mg), and in the presence of divalent transition metals (Mn, Cu, and Pd). Solid lines are spectra of high-molecular-weight fragments (>23 kbp), and broken lines are spectra of low-molecular-weight fragments (160 bp). Sample conditions include 55 mg DNA/ml, 100 mM divalent metal chloride, and 5 mM sodium cacodylate (pH 6.5) and a temperature of 11°C.

1240–1260 and at 1668 $cm^{-1}$. Similar perturbations are observed with thermal denaturation of B-DNA (Erfurth and Peticolas, 1975; Benevides et al., 1991). Other changes of frequency and intensity occur for the bands centered near 665–681, 727, 750, 1092, 1305–1380, 1489, and 1578 $cm^{-1}$.

## Nucleosomal DNA fragments (160 bp)

### *Complexes with alkaline earth metals*

Raman difference spectra are shown in Fig. 3. Perturbations caused by $Sr^{2+}$ are evidently weak, but $Ba^{2+}$, $Mg^{2+}$, and $Ca^{2+}$ produce significant spectral differences throughout the 1200–1500 $cm^{-1}$ region. In BaDNA, MgDNA, and CaDNA, the guanine N7 marker is clearly shifted to a frequency below its value (1489 $cm^{-1}$) in metal-free DNA, generating in each case a difference peak near 1480 $cm^{-1}$ and trough near 1495 $cm^{-1}$. The peak-to-trough intensity changes, which reflect the corresponding frequency shifts, are tabulated in column 5 of Table 1. Several additional bands in the intervals 1250–1450 and 750–950 $cm^{-1}$ are also perturbed, particularly for the CaDNA complex.

Fig. 3 shows further that, vis-à-vis metal-free DNA, the intensity distribution between 681 and 665 $cm^{-1}$ is unchanged in SrDNA and MgDNA and only marginally reduced in BaDNA and CaDNA. These data are compiled in column 8 of Table 1.

The difference peak at 774 $cm^{-1}$, which increases in amplitude in the order BaDNA < MgDNA < CaDNA (Fig. 3), is considered of marginal significance in view of the high intensity of the parent B-DNA band. A much larger intensity change in this spectral region accompanies the thermal denaturation of B-DNA (Erfurth and Peticolas, 1975). The alkaline earths also fail to generate any large intensity changes in the B-form marker band near 834 $cm^{-1}$. Table 1 (column 2) shows that more than 80% of the intensity near 834 $cm^{-1}$ is conserved in each complex (93% for MgDNA). Similarly, perturbations to the phosphodioxy band at 1092 $cm^{-1}$ are generally very small, except for MgDNA where the perturbation represents a 10% reduction in intensity. Previous studies (Aubrey et al., 1992; Stangret and Savoie, 1992) have reported similar effects of $Mg^{2+}$ on the intensity and shape of the phosphodioxy 1092 $cm^{-1}$ band. A structural model to explain the observed Raman perturbations has been proposed (Stangret and Savoie, 1992).

The characteristic Raman hypochromism of B-DNA (Small and Peticolas, 1971) provides, in principle, a number of Raman bands that can serve as candidates for monitoring denaturation of B-form secondary structure. For the present

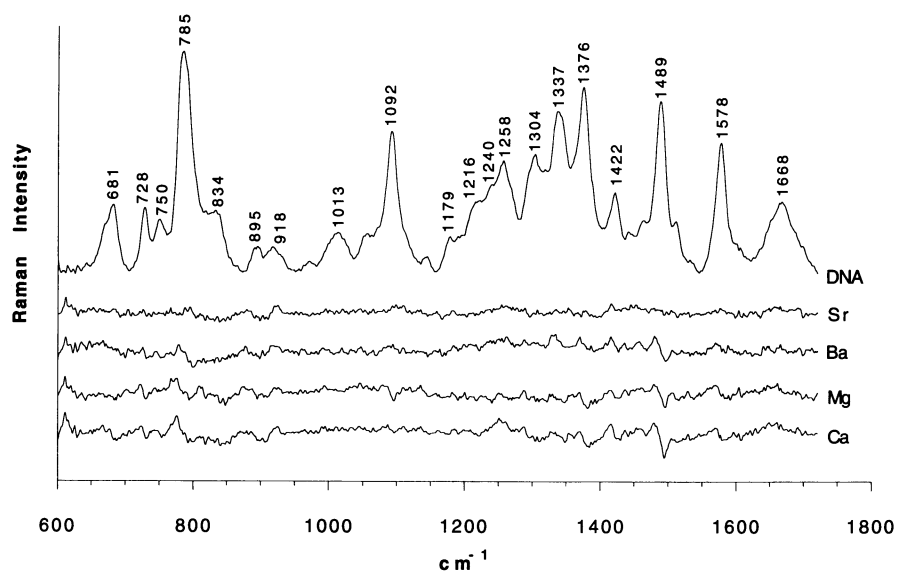


FIGURE 3 From top to bottom: Raman spectrum of 160 bp calf thymus DNA and the difference spectra obtained by its subtraction from spectra of the same DNA in the presence of the indicated alkaline earth metals. Other sample conditions are given in Fig. 1.

study, we found it most useful to select the metal-induced increase of intensity (hyperchromism) of the cytosine band at 1257 $cm^{-1}$ to monitor the degree of base unstacking with metal binding. (Most other bands in the 1200–1600 $cm^{-1}$ region undergo frequency shifts as well as intensity changes with metal binding, which complicates the measurement of their hyperchromic effects.) The percentage intensity change of the 1257 $cm^{-1}$ band is tabulated in column 4 of Table 1 and indicates relatively little unstacking of dC in these alkaline earth metal complexes of DNA.

Somewhat larger intensity perturbations (column 3, Table 1) were measured for the composite carbonyl band at 1668 $cm^{-1}$. These are expected to reflect changes in hydrogen bonding states of exocyclic donor and acceptor groups of the bases, as well as changes induced in the structure of water by the divalent cations (Benevides et al., 1988, 1991). In all alkaline earth metal complexes the 1668 $cm^{-1}$ band intensity change is 15% or less, suggesting relatively little change in base pairing of these B-DNA fragments.

### *Complexes with transition metals*

The Raman difference spectra shown in Fig. 4 reveal pronounced effects of the transition metals on the structure of 160 bp DNA. Virtually all Raman bands in the B-DNA spectrum are perturbed, and the magnitudes of the perturbations greatly exceed those induced by alkaline earth metal ions. (See preceding section.)

The spectroscopic measurements are compiled in Table 1. The B-form backbone geometry (column 2) is more than 20% diminished in all complexes (>50% for CoDNA); bands sensitive to base pairing (column 3) are significantly perturbed (36% for CoDNA); large hyperchromic effects (column 4) and significant N7 interactions (column 5) are also evident. We find evidence of direct binding of transition metals to adenine (column 6) and guanine (column 7) with the possibility of altered nucleoside conformations in dG residues (column 8). Again, these effects are most pronounced for CoDNA but are also significant for MnDNA, NiDNA, and CdDNA. Finally, all four of the transition metals monitored here exhibit evidence of strong interactions with DNA phosphates (column 10), in addition to the above noted strong interactions with purine residues. On the other hand, the Raman spectra suggest no specific interactions of the transition metal ions with dT residues (column 9). We may infer that the same is true of dC residues, since the dC markers (near 780 and 1257 $cm^{-1}$) exhibit their intensity changes without the anticipated frequency shifts that are characteristic of metal-base interaction (Lord and Thomas, 1967; Mansy et al., 1978; Moller et al., 1980). These considerations imply further that perturbations of the 1668 $cm^{-1}$ band (column 3) are the result not of interactions between transition metals and exocyclic groups (C=O, NH, $NH_2$) of dT and dC, but rather of interactions between the metal ions and exocyclic groups of dG and possibly also with the $NH_2$ group of dA.

In addition to the perturbations of marker bands listed in Table 1, we observe corresponding effects of the transition metal ions on Raman bands near 1240, 1304, 1337, 1376, and 1578 $cm^{-1}$ (Fig. 4), all of which are indicative of base unstacking. Our results are consistent with previous studies of divalent metal binding to model mononucleotides (Lord and Thomas, 1967; Mansy et al., 1978; Moller et al., 1980).

Fig. 4 and Table 1 (column 2) show that 160 bp DNA is significantly melted in the presence of $Mn^{2+}$, $Cd^{2+}$, and $Ni^{2+}$ and is very likely predominantly melted in the presence of $Co^{2+}$. The correspondence between perturbations of the 834 $cm^{-1}$ band (CoDNA > NiDNA > CdDNA and MnDNA) and 1668 $cm^{-1}$ band (CoDNA and CdDNA > NiDNA > MnDNA) is sufficiently close to suggest that these represent at least partly coupled processes associated with

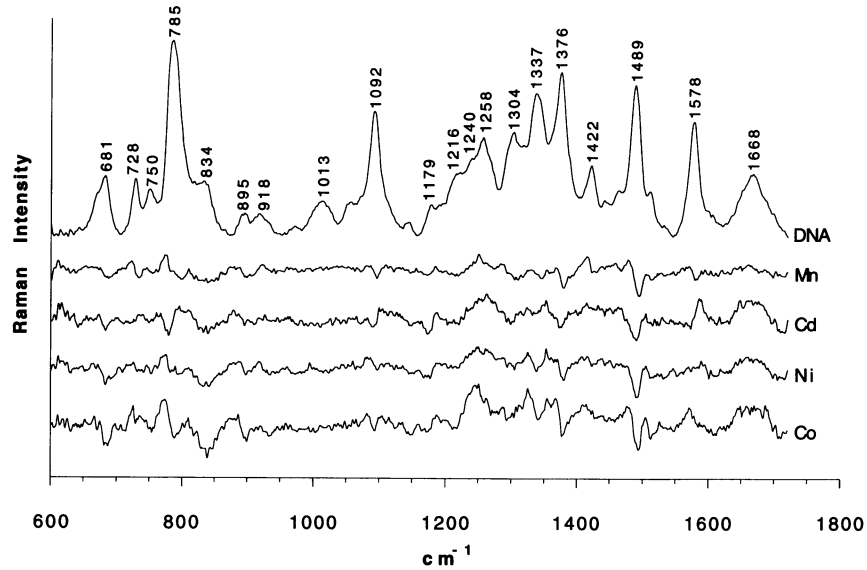


FIGURE 4 From top to bottom: Raman spectrum of 160 bp calf thymus DNA and the difference spectra obtained by its subtraction from spectra of the same DNA in the presence of the indicated divalent transition metals. Other sample conditions are given in Fig. 1.

denaturation of the double helix, that is, the former reflecting loss of ordered B-form backbone geometry and the latter reflecting altered base pairing. Such DNA denaturation is expected to make potential acceptor sites of the bases available for direct transition metal binding or chelation through the metal ion hydration sphere. Our results suggest that in 160 bp DNA, it is the ring sites of guanine (N7) and adenine (N1 and N7) and the exocyclic sites of guanine (6C=O, 1NH, $2NH_2$) that are the most likely targets of the transition metal ions.

## Genomic DNA fragments

### *Complexes with alkaline earth metals*

Effects of alkaline earth metal ions on the Raman spectrum of high-molecular-weight fragments (>23 kbp) of calf thymus DNA are shown in Fig. 5. Comparison with complexes of 160 bp DNA (cf. Fig. 3) shows that the Raman perturbations are qualitatively similar in the two cases. The Raman difference spectrum computed between the high- and low-molecular-weight DNA complex of each alkaline earth metal suggests that the structural effects of a given ion are similar for the two DNAs.

### *Complexes with transition metals*

Raman difference spectra of high-molecular-weight DNA are shown in Fig. 6 (Mn, Cd, Ni), Fig. 7 (Cu), and Fig. 8 (Pd). Comparisons with Fig. 4 indicate that the effects of these metals on the structure of >23 kbp DNA are of much greater magnitude than on 160 bp DNA. Additionally, for Cd we observe a more pronounced effect than reported previously (Langlais et al., 1990).

The results compiled in Table 1 show that more than 50% of the B-form backbone geometry (column 2) is eliminated in each complex (100% in the case of PdDNA). Comparably large changes occur in the bands sensitive to base pairing (column 3). Dramatic changes are also evident in the degree of base unstacking (columns 4 and 6) and extent of binding to N7 sites of dG residues (column 5). The results further imply nucleoside conformational changes (columns 7 and 8), which may be coupled to ligation of heavy metal cations at guanine acceptor sites. Table 1 (column 9) suggests further that $Cu^{2+}$ and $Pd^{2+}$ are significant perturbants of thymine ring structure, a characteristic not evident for any other divalent metal cation. Finally, these heavy metal cations are conspicuous perturbants of the DNA phosphodioxy groups (column 10).

The dramatic effects of $Pd^{2+}$ on numerous Raman bands of DNA (Fig. 8) imply complete denaturation of the B-form secondary structure. This can be attributed to the combined effects of both $Pd^{2+}$ and $H^+$ binding, since measurements on PdDNA were carried out at pH 1.8.

Heavy metal perturbation of the 1092 $cm^{-1}$ band, which is generally greater for >23 kbp DNA than for 160 bp DNA, is conspicuously large for the CuDNA complex. The significant shift to lower frequency observed for the phosphodioxy marker of CuDNA probably reflects direct interaction between $Cu^{2+}$ and/or $H^+$ with $PO_2^-$, resulting in electron withdrawal from the PO bonds with attendant reduction in the bond-stretching force constant.

The spectral region 1200–1600 $cm^{-1}$ in Figs. 6–8 reveals large intensity changes indicative of base unstacking and substantial frequency shifts indicative of specific metal-base interactions. The largest hyperchromicities are observed at 1239 $cm^{-1}$ for PdDNA; 1247 and 1263 $cm^{-1}$ for MnDNA, CdDNA, and NiDNA; and 1243 $cm^{-1}$ for CuDNA. These most likely represent superpositions of several overlapping intensity and frequency changes in bands from various DNA bases. For example, in CuDNA, the observed hyperchromicity near 1243 $cm^{-1}$ could reflect the composite effect of an intensity increase in the thymine component at 1240 $cm^{-1}$,

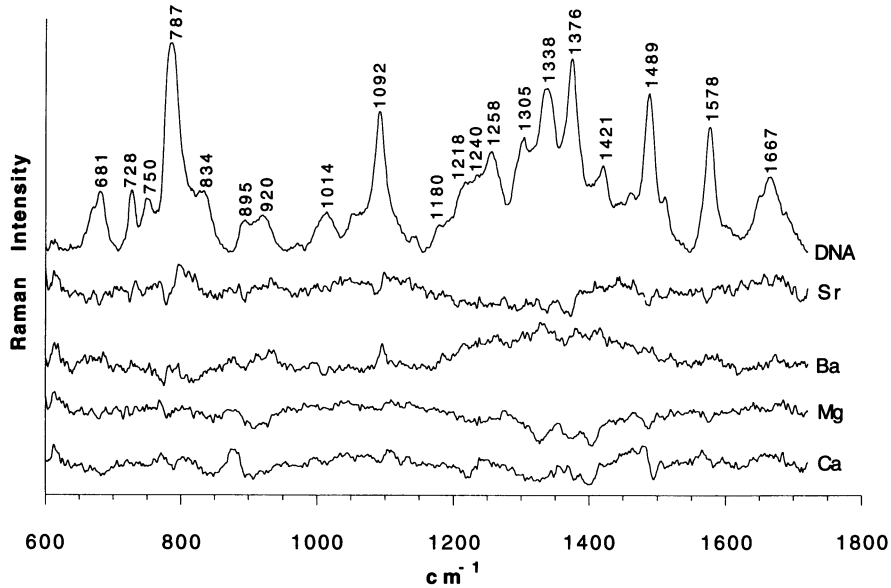


FIGURE 5 From top to bottom: Raman spectrum of >23 kbp calf thymus DNA and the difference spectra obtained by its subtraction from spectra of the same DNA in the presence of the indicated alkaline earth metals. Other sample conditions are given in Fig. 1.

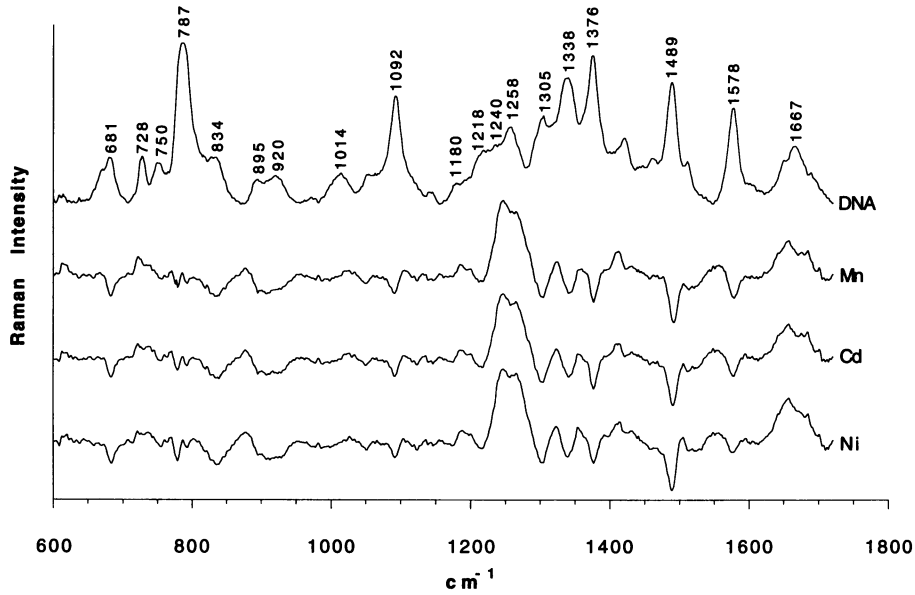


FIGURE 6 From top to bottom: Raman spectrum of >23 kbp calf thymus DNA and the difference spectra obtained by its subtraction from spectra of the same DNA in the presence of the indicated divalent transition metals. Other sample conditions are given in Fig. 1.

due to thymine base unstacking (Small and Peticolas, 1971), and an intensity increase in the cytosine component at 1257 $cm^{-1}$, due to metal binding at N3 (Lord and Thomas, 1967).

Raman bands of the bases at 1305, 1336, 1376, 1489, and 1578 $cm^{-1}$ exhibit roughly parallel behavior with binding of $Mn^{2+}$, $Cd^{2+}$, and $Ni^{2+}$ (Fig. 6), and these are similar to the perturbations observed with 160 bp DNA. The data are consistent with metal binding to N7 of guanine and to both N1 and N7 of adenine. In the cases of $Pd^{2+}$ and $Cu^{2+}$, the interpretation is complicated by pH effects that cause additional frequency shifts and by different relative intensities that suggest different modes of binding to the bases. At present, there are no model systems exhibiting similar behavior that would facilitate the more detailed interpretation of these results. Finally, we note that the binding of $Pd^{2+}$ and $Cu^{2+}$ may be sufficiently complex to generate two or more overlapping bands in the interval 1480–1490 $cm^{-1}$. Therefore, our results do not rule out the possibility of binding of $Pd^{2+}$ or $Cu^{2+}$ to more than one guanine acceptor site (e.g., N1 in addition to N7).

The 1668 $cm^{-1}$ band is greatly perturbed by all heavy metals, generating a shift of the band maximum to 1656 $cm^{-1}$. The collective evidence of decreased backbone order, extensive base unstacking, and metal ion binding to base ring and exocyclic sites normally involved in hydrogen bonding makes it clear that the B-DNA double helix is disrupted by these heavy metals.

## Correlations among marker bands

Each well-resolved Raman band of DNA corresponds to a distinctive normal mode of vibration localized within specific chemical groups of the macromolecule. The bands of primary interest in this study represent in-plane bond-

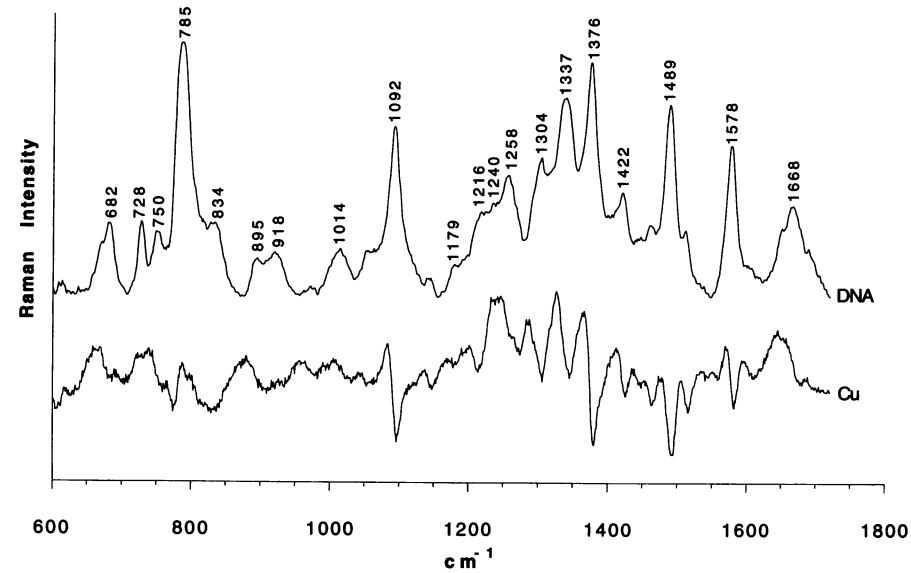


FIGURE 7 Raman spectrum of >23 kbp DNA (*top*) and the difference spectrum obtained by its subtraction from the spectrum of the same DNA in the presence of $CuCl_2$. Sample conditions include 55 mg DNA/ml, 100 mM $CuCl_2$, and 5 mM sodium cacodylate and a temperature of 11°C. Solution pH = 3.1.

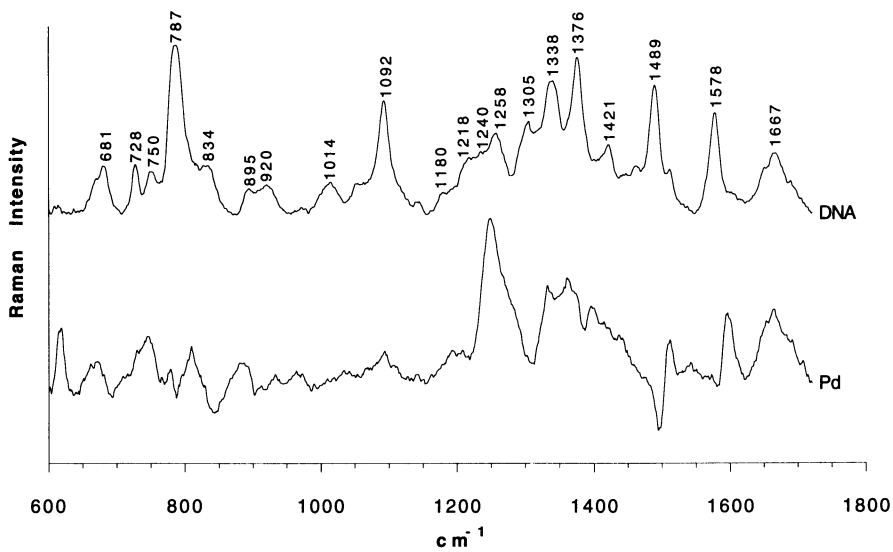


FIGURE 8 Raman spectrum of >23 kbp DNA (*top*) and the difference spectrum obtained by its subtraction from the spectrum of the same DNA in the presence of $PdCl_2$. Sample conditions include 55 mg DNA/ml, 100 mM $PdCl_2$ and 5 mM sodium cacodylate and a temperature of 11°C. Solution pH = 1.7.

stretching vibrations of a specific type of DNA base or its exocyclic substituents, or a bond-stretching vibration localized in the backbone (specifically in the phosphodioxy or phosphodiester groupings). In order to determine whether metal-induced perturbations of one band are correlated with perturbations of another, we investigated by use of correlation plots the perturbations observed in bands at 665, 681, 727, 750, 834, 1092, 1257, 1489, and 1668 $cm^{-1}$. The analysis was carried out for both 160 bp DNA and >23 kbp DNA. Both types of DNA gave evidence of strong linear correlations between most pairs of Raman bands. Representative plots are shown in Figs. 9 and 10, and a comprehensive tabulation is given in Table 2.

Fig. 9 shows the correlation between perturbations of intensities of bands at 1668 (thymine, guanine, and cytosine exocyclic groups) and 1257 $cm^{-1}$ (cytosine and adenine rings) for both DNAs. The relationship is seen to be highly linear, with a correlation coefficient of 0.96. We interpret this result to indicate a direct relationship between base unpairing, manifested by a breaking of hydrogen bonds associated with base exocyclic groups, and base unstacking. Note that the changes observed in the 1668 and 1257 $cm^{-1}$ bands are much greater for the heavy metals than for the alkaline earths. Fig. 10 shows the corresponding correlation between base unstacking (1257 $cm^{-1}$) and the percentage reduction in B-form backbone geometry (correlation coefficient = 0.97). Other correlation coefficients are listed in Table 2. The structural information content of Table 2 is summarized in Table 3.

The correlations of Table 2 show, for example, that the metal-induced elimination of B-form backbone geometry (834 $cm^{-1}$ marker) is linked with base unstacking (hyperchromicities near 727 and 1257 $cm^{-1}$) and base unpairing (1668 $cm^{-1}$ marker), a pattern consistent with DNA melting. On the other hand, a linkage between any of these band perturbations and the phosphodioxy marker at 1092 $cm^{-1}$ is much weaker. The latter is not surprising, in view of the fact that electrostatic interactions generally do not strongly perturb Raman bands associated with vibrational modes localized in the charged groups. At the conditions employed for the present experiments ($[M^{2+}]/[PO_2^-] = 0.6$), interactions between the divalent metal cations and the phosphodioxy anions should be dominated by electrostatics. $Cu^{2+}$, however, would appear to be an exception.

The apparently strong correlation (Table 2) between metal interaction with guanine N7 sites (1489 $cm^{-1}$ marker) and the position of the dG marker at 665 $cm^{-1}$ is also informative. It indicates either (*a*) that metal ligation at N7 destabilizes the C2′-*endo*/*anti* dG conformation or, more probably, (*b*) that metal complexation with the imidazole ring moiety of guanine strongly perturbs the electronic structure within the six-membered ring, thus shifting the dG marker to lower frequency. This would be consistent with a reduction in $\pi$-electron density within the six-membered ring as a consequence of electrophilic attack at N7.

## DISCUSSION

Table 1 lists the major perturbations to the Raman spectrum of B-DNA induced by a variety of divalent metal cations. Results for both low-molecular-weight (160 bp) and high-molecular-weight (>23 kbp) DNA are included. The structural significance of these changes is summarized in Table 3. Collectively, our results indicate the following decreasing order for the strength of metal-ion interaction with DNA bases: $Pd^{2+} > Cu^{2+}$, $Co^{2+} > Ni^{2+}$, $Cd^{2+}$, $Mn^{2+} > Ca^{2+} > Mg^{2+}$, $Sr^{2+}$, $Ba^{2+}$. Except for $Co^{2+}$, the order manifested in the Raman data is consistent with the order determined by other methods for measuring cation destabilization of B-DNA. Perturbations induced in the B-DNA Raman spectrum are clearly greater for transition metals than for alkaline earth metals. This may be attributed to the unfilled *d* orbitals of the former, which can lead to covalent complexes between the metal ion and the DNA bases, a type of linkage that is expected to profoundly alter the electronic distribution within the heterocycle and thus greatly perturb the Raman

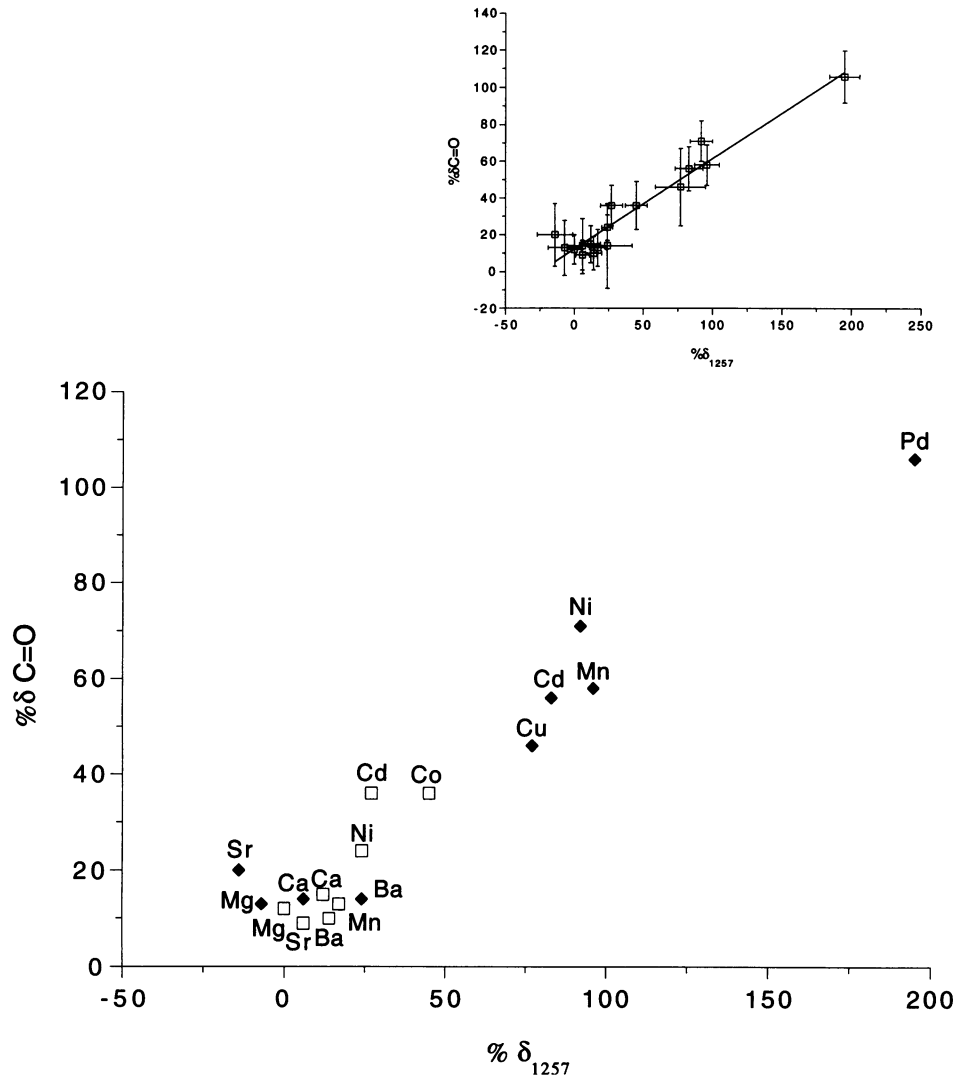


FIGURE 9 Correlation plots for the percentage change in the carbonyl band (%δ C=O) and the percentage change in the 1257 $cm^{-1}$ band ($\%\delta_{1257}$) of DNA in the presence of different divalent metal cations. Data are shown for >23 kbp DNA (◆) and 160 bp DNA (□) for which a linear correlation coefficient of 0.96 was calculated. The inset shows the margins of error (Table 1) associated with each data point.

fingerprint of the base. Such unfilled *d* orbitals are lacking in the alkaline earth metals.

Insoluble "aggregates" were detected visually for each of the DNA-metal complexes that exhibited Raman spectroscopic evidence of melting. The spectroscopic and visual evidence linked melting with aggregation even at temperatures as low as 11°C. Several studies have previously addressed aggregation of DNA in the presence of divalent metal cations (Stevens and Duggan, 1957; Yurgaitis and Lazurkin, 1981). These also confirm a close correspondence between thermal- and metal-induced melting. Conversely, we observed no aggregation for those DNA complexes that lacked Raman evidence of melting, such as alkaline earth metal complexes and selected transition metal complexes of nucleosomal DNA fragments.

A statistical mechanical treatment of the relationship between DNA aggregation and thermal denaturation (Shibata and Schurr, 1981) suggests the formation of multistranded complexes, an association phenomenon that depends also on DNA chain length. To explain the effects of the different divalent metal cations, we propose that they bind specifically and characteristically to DNA base sites. The Raman evidence indicates that purine N7 acceptors are the most probable metal-binding sites. Secondary chelation sites involving the exocyclic acceptors (C=O, NH, $NH_2$) are also indicated by the Raman data. Metal binding at the primary sites is proposed to locally destabilize the double helix. As a result, the bases are displaced relative to the helix axis, that is, the base pairs swing open and furnish additional electron-rich sites, such as the N1 acceptor of adenine, N1H of guanine, N3 of cytosine, and N3H of thymine, allowing further binding of metal ions. The metal-bound bases may then serve as additional nucleation sites to link with other available base acceptors. This mechanism would allow separated DNA strands, or their separated local domains, to crosslink. Extension of the crosslinking would lead eventually to a net-

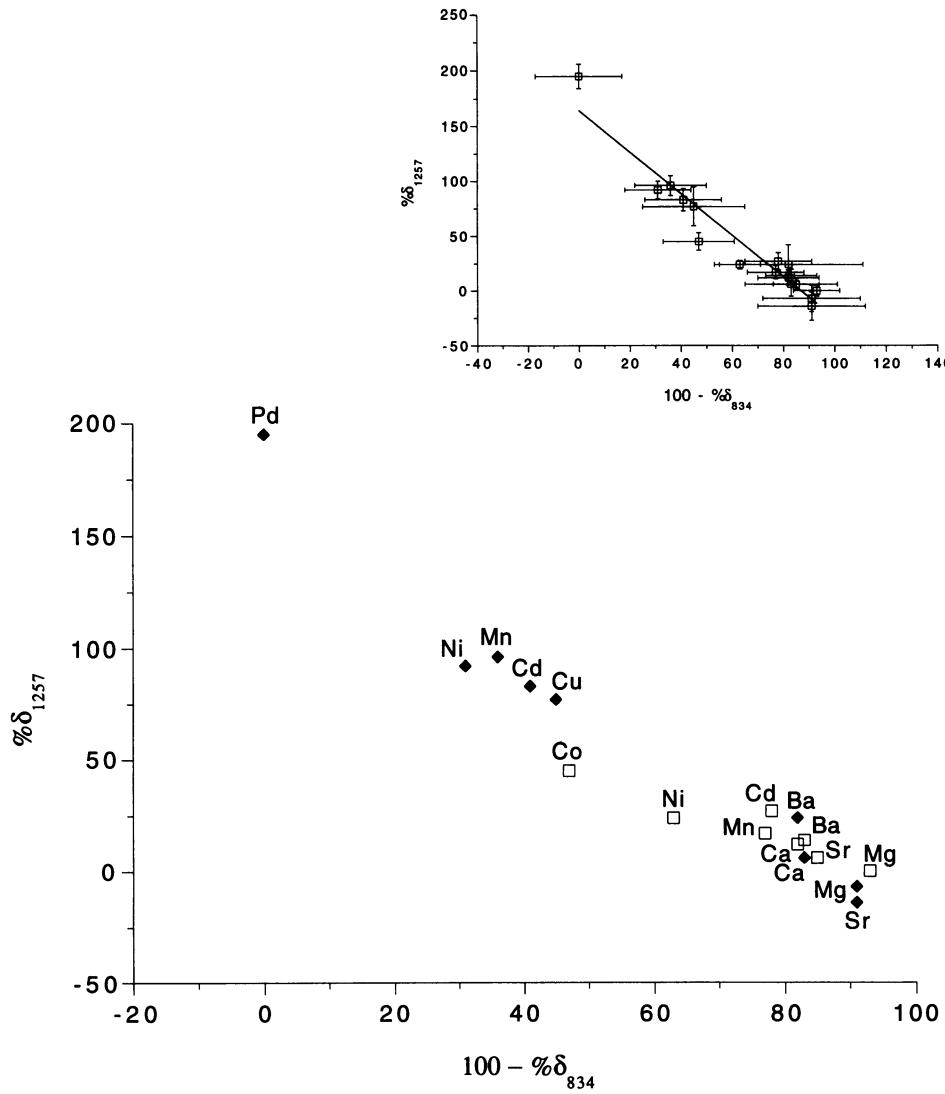


FIGURE 10 Correlation plots for the percentage change in the 1257 $cm^{-1}$ band ($\%\delta_{1257}$) and the percentage change in the 834 $cm^{-1}$ band ($100 - \%\delta_{834}$) of DNA in the presence of divalent metal cations. Data are shown for >23 kbp DNA (♦) and 160 bp DNA (□) for which a linear correlation coefficient of 0.97 was calculated. The inset shows the margins of error (Table 1) associated with each data point.

**TABLE 2 Correlation coefficients for DNA Raman band perturbations in divalent metal complexes***

| | Backbone $100-\%\delta_{834}$ | C=O $\%\delta C{=}O$ | dC $\%\delta_{1257}$ | dG,dA $\lvert\%\delta_{1489}\rvert$ | dA $\%\delta_{727}$ | dG $\delta\sigma_{681}$ | dG $I_{681}/I_{665}$ | dT $\%\delta_{750}$ | $PO_2$ $\lvert\%\delta_{1092}\rvert$ |
|---|---|---|---|---|---|---|---|---|---|
| $100-\%\delta_{834}$ | — | **0.95** | **0.97** | **0.94** | **0.94** | **0.93** | **0.93** | 0.53 | 0.53 |
| $\%\delta C{=}O$ | | — | **0.96** | **0.93** | **0.90** | **0.89** | **0.84** | 0.58 | 0.52 |
| $\%\delta_{1257}$ | | | — | **0.94** | **0.95** | **0.91** | **0.86** | 0.63 | 0.53 |
| $\lvert\%\delta_{1489}\rvert$ | | | | — | **0.90** | **0.94** | **0.89** | 0.63 | 0.64 |
| $\%\delta_{727}$ | | | | | — | **0.88** | **0.87** | 0.69 | 0.51 |
| $\delta\sigma_{681}$ | | | | | | — | **0.97** | 0.49 | 0.73 |
| $I_{681}/I_{665}$ | | | | | | | — | 0.47 | 0.70 |
| $\%\delta_{750}$ | | | | | | | | — | 0.35 |
| $\lvert\%\delta_{1092}\rvert$ | | | | | | | | | — |

* Column and row headings are as defined in Table 1. The most significant correlations (>0.85) are in bold type.

work of DNA aggregates and ultimately to an insoluble complex. Since DNA aggregation is dependent initially upon local melting, the metal cations exhibiting higher affinities for DNA bases (especially purine N7 sites) would favor greater aggregation.

The above model also explains the consistency between the order of effectiveness of divalent cations in inducing DNA melting (Eichhorn and Shin, 1968) and the phenomenon of aggregation at elevated temperatures (Knoll et al., 1988). Yurgaitis and Lazurkin (1981) have shown that as

**TABLE 3 Effect of metal-ion binding on DNA Raman bands**

| Band ($cm^{-1}$) | Group | Effect observed | Interpretation |
|---|---|---|---|
| 665 | dG | Intensity increase | Increase of C3′-endo/anti-dG |
| 668 | dT | Intensity increase | Increase of C2′-endo/anti-dT |
| 682 | dG | Intensity decrease | Decrease of C2′-endo/anti-dG |
| 727 | dA | Intensity increase | Unstacking of dA |
| 750 | dT | No consistent pattern* | |
| 834 | COPOC | Intensity decrease | Loss of B-form backbone |
| 1092 | $PO_2^-$ | No consistent pattern‡ | |
| 1240 | dT | Intensity increase | Unstacking of dT |
| 1257 | dC | Intensity increase | Unstacking of dC |
| 1489 | dG | Intensity decrease & low-frequency shift | Metal coordination at N7 |
| 1668 | C=O | Intensity increase & low-frequency shift | Unpairing of bases (T, G, C) |

* The band is not highly sensitive to structural changes other than the B → A transition of DNA (Thomas and Benevides, 1985).
‡ The band is diminished by protonation of the phosphodioxy group at low pH but undergoes more complex changes with binding of different metal cations (Stangret and Savoie, 1992).

DNA strands begin to melt upon heating, aggregation occurs in the presence of $Mn^{2+}$. Similarly, Stevens and Duggan (1957) have demonstrated the formation of an insoluble precipitate upon heating DNA in the presence of $Pb^{2+}$. Evidence of melted aggregates of DNA and RNA has also been reported at 4°C in the presence of divalent metal cations (Eisinger et al., 1963; Lin and Chargaff, 1966). Knoll et al. (1988) have shown that DNA aggregates formed in the presence of $Mg^{2+}$, $Ca^{2+}$, or $Mn^{2+}$ are resistant to S1 nuclease. This suggests that aggregates are only partially denatured and that removal of the divalent metal cations may allow reformation of an intact double helix. In fact DNA heated in the presence of divalent metal cations disaggregates upon addition of EDTA, and this disaggregation is accompanied by hypochromism at 260 nm (Knoll et al., 1988).

A partially denatured and aggregated state of DNA in the presence of divalent cations is reminiscent of P-DNA (Johnson and Girod, 1974; Zehfus and Johnson, 1981, 1984), which is also capable of reforming an intact double helix. There are, however, distinct differences between these DNA forms; the P-DNA structure is generated with high concentrations of ethanol or methanol present in the aqueous solvent and occurs in the absence of divalent metal cations.

The generation of P-DNA in hydrophobic solvents and of DNA aggregates in the presence of divalent cations may reflect a general phenomenon associated with a reduction in the local activity of water at major groove sites and in the vicinity of phosphate groups of B-DNA. Similar environmental conditions may favor the condensation of native DNA in biological assemblies, including chromatin and viruses. Further characterization of the structures and stabilities of these altered states of DNA is required. In a forthcoming paper we shall report and compare the thermostabilities of NiDNA and CdDNA, as probed by Raman spectroscopy, calorimetry, and potentiometry.

This research was supported by National Institutes of Health grants GM28093 (V. A. B.) and AI18758 (G. J. T.).
J. Duguid was the recipient of a Molecular Biophysics Predoctoral Traineeship from the National Institutes of Health (GM08277) and acknowledges the assistance of R. Becka and K. Reilly (UMKC), D. Knoll (Kallestad Laboratories, Chaska, MN), and P. Arscott (University of Minnesota) during various stages of this work.

## REFERENCES

Aubrey, K. L., S. R. Casjens, and G. J. Thomas, Jr. 1992. Secondary structure and interactions of the packaged dsDNA genome of bacteriophage P22 investigated by Raman difference spectroscopy. *Biochemistry*. 31: 11835–11842.

Benevides, J. M., P. L. Stow, L. L. Ilag, N. L. Incardona, and G. J. Thomas, Jr. 1991. Differences in secondary structure between packaged and unpackaged single-stranded DNA of bacteriophage ψX174 determined by Raman spectroscopy: a model for ψX174 DNA packaging. *Biochemistry*. 30:4855–4863.

Benevides, J. M., A. H-J. Wang, G. A. van der Marel, J. H. van Boom, A. Rich, and G. J. Thomas, Jr. 1984. The Raman spectra of left-handed DNA oligomers incorporating adenine-thymine base pairs. *Nucleic Acids Res.* 12:5913–5925.

Benevides, J. M., A. H-J. Wang, G. A. van der Marel, J. H. van Boom, and G. J. Thomas Jr. 1988. Crystal and solution structures of the B-DNA dodecamer d(CGCAAATTTGCGC) probed by Raman spectroscopy: heterogeneity in the crystal structure does not persist in the solution structure. *Biochemistry*. 27:931–938.

Chang, D-K., and D. R. Kearns. 1986. Distribution of $Mn^{2+}$ ions around poly(rI)·poly(rC). *Biopolymers*. 25:1283–1297.

Clement, R. M., J. Sturm, and M. P. Daune. 1973. Interaction of metallic cations with DNA. VI. Specific binding of $Mg^{++}$ and $Mn^{++}$. *Biopolymers*. 12:405–421.

Day, L. A., A. Casadevall, B. Prescott, and G. J. Thomas, Jr. 1988. Raman spectroscopy of mercury(II) binding to two filamentous viruses: Ff(fd, M13, f1) and Pf1. *Biochemistry*. 27:706–711.

Dix, D. E., and D. B. Strauss. 1972. DNA helix stability. 1. Differential stabilization by counter cations. *Arch. Biochem. Biophys.* 152:299–310.

Dove, W. F., and N. Davidson. 1962. Cation effects on the denaturation of DNA. *J. Mol. Biol.* 5:467–478.

Eichhorn, G. L., and P. Clark. 1965. Interactions of metal ions with polynucleotides and related compounds. V. The unwinding and rewinding of DNA strands under the influence of copper(II) ions. *Proc. Natl. Acad. Sci. USA*. 53:586–593.

Eichhorn, G. L., and Y. A. Shin. 1968. Interaction of metal ions with polynucleotides and related compounds. XII. The relative effect of various metal ions on DNA helicity. *J. Am. Chem. Soc.* 90:7323–7328.

Eisinger, J., F. Fawaz-Estrup, and R. G. Shulman. 1963. Precipitation of synthetic polynucleotides by $Mg^{2+}$. *Biochim. Biophys. Acta*. 72:120–122.

Erfurth, S. C., and W. L. Peticolas. 1975. Melting and premelting phenomena in DNA by laser Raman scattering. *Biopolymers*. 14:247–264.

Erfurth, S. C., E. J. Kiser, and W. L. Peticolas. 1972. Determination of the backbone structure of nucleic acid oligomers by laser Raman scattering. *Proc. Natl. Acad. Sci. USA*. 69:938–941.

Gessner, R. V., G. J. Quigley, A. H-J. Wang, G. A. van der Marel, J. H. van Boom, and A. Rich. 1985. Structural basis for stabilization of Z-DNA by cobalt hexammine and magnesium cations. *Biochemistry*. 24:237–240.

Granot, J., and D. R. Kearns. 1982. Interactions of DNA with divalent metal ions. II. proton relaxation enhancement studies. *Biopolymers*. 21: 203–218.

Granot, J. H., J. Feigon, and D. R. Kearns. 1982. Interactions of DNA with divalent metal ions. I. $^{31}$P-NMR studies. *Biopolymers*. 21:181–201.

Hardin, C. C., T. Watson, M. Corregan, and C. Bailey. 1992. Cation-dependent transition between the quadruplex and Watson-Crick hairpin forms of d(CGCG3GCG). *Biochemistry*. 31:833–841.

Johnson, W. C., Jr., and J. C. Girod. 1974. A novel denaturation of DNA. *Biochim. Biophys. Acta*. 353:193–199.

Jovin, T. M., L. P. McIntosh, D. J. Arndt-Jovin, D. A. Zarling, M. Robert-Nicoud, J. H. van de Sande, K. F. Jorgenson, and F. Eckstein. 1983. Left-handed DNA: from synthetic polymers to chromosomes. *J. Biomol. Struct. Dyn.* 1:21–57.

Jovin, T. M., D. M. Soumpasis, and L. P. McIntosh. 1987. The transition between B-DNA and Z-DNA. *Annu. Rev. Phys. Chem.* 38:521–560.

Keller, P. B., and K. A. Hartman. 1986. The effect of ionic environment and mercury(II) binding on the alternative structures of DNA. An infrared spectroscopic study. *Spectrochim. Acta*. 42A:299–306.

Keller, P. B., and K. A. Hartman. 1987. Structural forms and transitions for the complex of mercury(II) with poly(dG-dC). *J. Biomol. Struct. Dyn.* 4:1013–1026.

Keller, P. B., D. M. Loprete, and K. A. Hartman. 1988. Structural forms and transitions of poly(dG-dC) with Cd(II), Ag(I) and $NaNO_3$. *J. Biomol. Struct. Dyn.* 5:1221–1229.

Kennedy, S. D., and R. G. Bryant. 1986. Manganese-deoxyribonucleic acid binding modes. *Biophys. J.* 50:669–676.

Knoll, D. A., M. G. Fried, and V. A. Bloomfield. 1988. Heat-induced DNA aggregation in the presence of divalent metal salts. *In* Structure and Expression: DNA and Its Drug Complexes. Vol. 2, M. H. Sarma and R. H. Sarma, editors. Adenine Press, Albany, NY. pp. 123–146.

Lamba, O. P., R. Becka, and G. J. Thomas, Jr. 1990. Adenine and guanine 8CH exchange in nucleic acids: resolution and measurement by Raman optical multichannel analysis. *Biopolymers*. 29:1465–1477.

Langlais, M., H. A. Tajmir-Riahi, and R. Savoie. 1990. Raman spectroscopic study of the effects of $Ca^{2+}$, $Mg^{2+}$, $Zn^{2+}$ and $Cd^{2+}$ ions on calf thymus DNA: binding sites and conformational changes. *Biopolymers*. 30:743–752.

Lin, H. J., and E. Chargaff. 1966. On the denaturation of deoxyribonucleic acid. *Biochim. Biophys. Acta*. 123:66–75.

Lord, R. C., and G. C. Thomas, Jr. 1967. Raman studies of nucleic acids. II. Aqueous purine and pyrimidine mixtures. *Biochim. Biophys. Acta*. 142:1–11.

Luck, G., and C. Zimmer. 1972. Conformational aspects and reactivity of DNA: effects of manganese and magnesium ions on interaction with DNA. *Eur. J. Biochem.* 29:528–536.

Mansy, S., G. Y. H. Chu, R. E. Duncan, and R. S. Tobias. 1978. Heavy metal nucleotide interactions. 12. Competitive reactions in systems of four nucleotides with *cis*- or *trans*-diamineplatinum(II). Raman difference spectrophotometric determination of the relative nucleophilicity of guanosine, cytidine, adenosine and uridine monophosphates as well as the analogous bases in DNA. *J. Am. Chem. Soc.* 100:607–616.

Moller, M. R., M. A. Bruck, T. O'Connor, F. J. Armatis Jr., E. A. Knolinski, N. Kottmair, and R. S. Tobias. 1980. Heavy metal-nucleotide interactions. 14. Raman difference spectrophotometric studies of competitive reactions in mixtures of four nucleotides with the electrophiles methylmercury(II) perchlorate, *cis*-dimethylgold(III) perchlorate, dichloroethylene-diamine-palladium(II), *trans*-dichlorodiaminepalladium(II) and aquopentaaminecobalt(III) perchlorate. Factors governing selectivity in the binding reactions. *J. Am. Chem. Soc.* 102:4589–4598.

Prescott, B., W. Steinmetz, and G. J. Thomas, Jr. 1984. Characterization of DNA structures by laser Raman spectroscopy. *Biopolymers*. 23:235–256.

Rose, D. M., M. L. Bleam, M. T. Record, Jr., and R. G. Bryant. 1980. $^{25}$Mg NMR in DNA solutions: dominance of site binding effects. *Proc. Natl. Acad. Sci. USA*. 77:6289–6292.

Rose, D. M., C. F. Polnaszek, and R. G. Bryant. 1982. $^{25}$Mg-NMR investigations of the magnesium ion-DNA interaction. *Biopolymers*. 21: 653–664.

Shibata, J. H., and J. M. Schurr. 1981. A theory of aggregation in the thermal denaturation region of multistrand biopolymers. *Biopolymers*. 20: 525–549.

Shin, Y. A., and G. L. Eichhorn. 1968. Interactions of metal ions with polynucleotides and related compounds. XI. The reversible unwinding and rewinding of deoxyribonucleic acid by zinc(II) ions through temperature manipulation. *Biochemistry*. 7:1026–1032.

Sissf, I., J. Grisvard, and E. Guille. 1976. Studies on metal ions-DNA interactions: specific behavior of reiterative DNA sequences. *Prog. Biophys. Mol. Biol.* 31:165–199.

Small, E. W., and W. L. Peticolas. 1971. Conformational dependence of the Raman scattering intensities from polynucleotides. *Biopolymers*. 10: 69–88.

Stangret, J., and R. Savoie. 1992. Vibrational spectroscopic study of the interaction of metal ions with diethyl phosphate, a model for biological systems. *Can. J. Chem.* 70:2875–2883.

Stevens, V. L., and E. L. Duggan. 1957. Deformation of deoxyribonucleate. II. Precipitation of heat-deformed DNA with millimolar lead ion. *J. Am. Chem. Soc.* 79:5703–5706.

Strzelecka, T. E., and R. L. Rill. 1987. Solid-state $^{31}$P NMR studies of DNA liquid crystalline phases. Isotropic to cholesteric transition. *J. Am. Chem. Soc.* 109:4513–4518.

Tajmir-Riahi, H. A., M. Langlais, and R. Savoie. 1988. A laser Raman spectroscopic study of the interaction of calf-thymus DNA with Cu(II) and Pb(II) ions: metal ion binding and DNA conformational changes. *Nucleic Acids Res.* 16:751–762.

Theophanides, T., and H. A. Tajmir-Riahi. 1985. Flexibility of DNA and RNA upon binding to different metal cations. An investigation of the B to A to Z conformational transition by Fourier transform infrared spectroscopy. *J. Biomol. Struct. Dyn.* 2:995–1004.

Thomas, G. J., Jr., and J. M. Benevides. 1985. An A-helix structure for poly(dA-dT)·poly(dA-dT). *Biopolymers*. 24:1101–1105.

Thomas, G. J., Jr., and A. H-J. Wang. 1988. Laser Raman spectroscopy of nucleic acids. *Nucleic Acids Mol. Biol.* 2:1–30.

Van Steenwinkel, R., F. Campagnari, and M. Merlini. 1981. Interaction of $Mn^{2+}$ with DNA as studied by proton-relaxation enhancement of solvent water. *Biopolymers*. 20:915–923.

Votavov, H., D. Kucerov, J. Felsberg, and J. Sponar. 1986. Changes in conformation, stability and condensation of DNA by univalent and divalent cations in methanol-water mixtures. *J. Biomol. Struct. Dyn.* 4:477–489.

Wang, L., M. Ferrari, and V. A. Bloomfield. 1990. Large-scale preparation of mononucleosomal DNA from calf thymus for biophysical studies. *Biotechniques*. 9:24–27.

Wilson, R. W., and V. A. Bloomfield. 1979. Counterion-induced condensation of deoxyribonucleic acid. A light-scattering study. *Biochemistry*. 18:2192–2196.

Woisard, A., G. V. Fazakerley, and W. Guschlbauer. 1985. Z-DNA is formed by poly(dC-dG) and poly(dm5C-dG) at micro or nanomolar concentrations of some zinc(II) and copper(II) complexes. *J. Biomol. Struct. Dyn.* 2:1205–1220.

Yamane, T., and N. Davidson. 1961. On the complexing of deoxyribonucleic acid (DNA) by mercuric ion. *J. Am. Chem. Soc.* 83:2599–2607.

Yurgaitis, A. P., and Y. S. Lazurkin. 1981. Mechanism of DNA denaturation in the presence of manganese ions. *Biopolymers*. 20:967–975.

Zehfus, M. H., and W. C. Johnson, Jr. 1981. Properties of P-form DNA as revealed by circular dichroism. *Biopolymers*. 20:1589–1603.

Zehfus, M. H., and W. C. Johnson, Jr. 1984. Conformation of P-form DNA. *Biopolymers*. 23:1269–1281.

Zimmer, C., G. Luck, and H. Triebel. 1974. Conformation and reactivity of DNA. IV. Base binding ability of transition metal ions to native DNA and effect on helix conformation with special reference to DNA-Zn(II) complex. *Biopolymers*. 13:425–453.